J Nanopart Res (2011) 13:4957–4968
DOI 10.1007/s11051-011-0476-y

RESEARCH PAPER

Synthesis of gold nanoparticles by *Cacumen Platycladi* leaf extract and its simulated solution: toward the plant-mediated biosynthetic mechanism

Guowu Zhan · Jiale Huang · Liqin Lin · Wenshuang Lin · Kamana Emmanuel · Qingbiao Li

Received: 3 August 2010 / Accepted: 22 June 2011 / Published online: 9 July 2011

Abstract In this study, biogenic fabrication of gold nanoparticles (AuNPs), respectively, by *Cacumen Platycladi* leaf extract and the simulation of its active components were thoroughly investigated. The simulated solution was prepared based on components measurement and Fourier-transform infrared spectroscopy analysis of *Cacumen Platycladi* leaf extract before and after reaction. Several analytic methods such as UV–Vis spectrophotometry, X-ray diffraction, transmission electron microscopy, and thermogravimetric study were adopted to characterize the AuNPs. The results showed that flavonoid and reducing sugar were the main reductive and protective components in the extract vital in the biosynthesis of the AuNPs. In addition, pH of the reaction solution was proved to be the most significant factor upon the synthesis process. The bioreduction mechanism of chloroaurate ions and the formation mechanism of AuNPs were also discussed. To the best of our knowledge, this is the first report on plausible elucidation of the biosynthetic mechanism through comparative study between a plant extract and its simulated solution.

Keywords Gold · Nanoparticles · Biosynthesis · Mechanism Comparable study · Nanobiotechnology

G. Zhan · J. Huang · L. Lin · W. Lin · K. Emmanuel · Q. Li (✉)
Department of Chemical and Biochemical Engineering, Xiamen University, Xiamen 361005, China
e-mail: kelqb@xmu.edu.cn

G. Zhan · J. Huang · L. Lin · W. Lin · K. Emmanuel · Q. Li
National Engineering Laboratory for Green Chemical Productions of Alcohols-Ethers-Esters, Xiamen University, Xiamen 361005, China

G. Zhan · J. Huang · L. Lin · W. Lin · K. Emmanuel · Q. Li
Key Lab for Chemical Biology of Fujian Province, Xiamen University, Xiamen 361005, China

Introduction

Currently, nanoparticles (NPs) have drawn tremendous attention because of their valuable properties on optical, electronic, medical, sensor, and catalytic application (Brust et al. 1998; Daniel and Astruc 2004; Shipway et al. 2000). The synthesis and characterization of NPs have emerged as an important branch of nanotechnology in the last decade, particularly for noble metals (such as Au, Pd, Pt, and Ag). Either chemical or physical approaches are usually employed to synthesize metal NPs because of their inherent advantage in producing well-defined NPs with fairly controllable shapes and sizes (Xia et al. 2009). However, the former methods involve tedious treatments, such as microemulsion (Pal et al. 2007), laser photolysis (Jin et al. 2001), hydrothermal induction (Yu and Yam 2005), or toxic chemical

reduction, besides auxiliary capping agents or templates (Lu et al. 2008), while the latter methods are dependent on costly physical techniques and equipments (Fitz-Gerald et al. 1999). Driven by the growing impetus of green chemistry, fabrication of NPs utilizing biological organisms would be a better alternative to conventional chemical and physical methods. In general, biological organisms refer to microorganisms, plant biomass or plant extracts which represent a process of cost-effective and environmentally benign manner (Mohanpuria et al. 2008). Nevertheless, subsequent separation of NPs formed with microorganisms intracellularly is usually difficult (Gericke and Pinches 2006), and microorganisms used for extracellular biosynthesis needs extensive screening (Labrenz et al. 2000). On the contrary, plant-mediated biosynthesis of NPs has attracted much attention as they conveniently produce NPs extracellularly. Moreover, the use of plant biomass and extract can circumvent the laborious cultivation of microorganisms (Shankar et al. 2003b).

Following the pioneering study of Gardea-Torresdey et al. (1999) on plant-mediated biosynthesis of gold NPs (AuNPs), many efforts have been directed toward this area with the use of plants, such as *Geranium* (Shankar et al. 2003a), *Wheat* (Armendariz et al. 2004), *Lemongrass* (Shankar et al. 2004), *Sargassum sp.* (Liu et al. 2005), *Hop* (Lopez et al. 2005), *Emblica officianalis* (Ankamwar et al. 2005), *Aloe vera* (Chandran et al. 2006), *Cinnamomum camphora* (Huang et al. 2007), *Coriander* (Narayanan and Sakthivel 2008), *Phyllanthus amarus* (Kasthuri et al. 2009), and so on. Very recently, Anuradha et al. (2010) used the extract of *Azadirachta indica* for the synthesis of AuNPs with uniform shape and size at ambient temperature. Singh et al. (2010) reported a simple way for preparing AuNPs using clove extract, where the shape and size of AuNPs were highly affected by the ratio of $HAuCl_4$ to clove extract. According to these synthetic procedures, AuNPs can be easily obtained by simply mixing the gold precursors and the plant extract together. However, the detailed mechanism of this redox process remains unclear because of the complicated components of plant biomass. Based on Fourier-transform infrared spectroscopy (FTIR) analysis of the plant biomass, $-OCH_3$ groups, in *Phyllanthin* extract (Kasthuri et al. 2009), eugenol in *clove* extract (Singh et al. 2010), and polyol components in *Cinnamomum camphora* leaf extract (Huang et al. 2007) were demonstrated to be responsible for the formation and stabilization of AuNPs. Yet, the elucidation of the mechanisms of these novel biosynthesis processes remains a challenge and needs much effort and exploration from researchers.

In this study, AuNPs were biologically synthesized by *Cacumen Platycladi* (*C. Platycladi*) leaf extract. In an attempt to explore the mechanism underlying this biosynthesis process, a simulated solution of the active components was prepared by mixing several known chemical substances based on components measurement and FTIR analysis of *C. Platycladi* leaf extract before and after reaction. Then, the simulated solution was adopted for the synthesis of AuNPs. The resulting AuNPs were characterized using UV–Vis spectra, thermogravimetric (TG) study, X-ray diffraction (XRD) patterns, and transmission electron microscopy (TEM) analyses. The residual chloroaurate ions were monitored by atomic absorption spectrophotometry (AAS) to examine the conversion of chloroaurate ions. Subsequently, the effects of reaction temperature and pH of the reaction solution on the morphology, size, and size distribution of AuNPs were thoroughly studied using TEM observation and UV–Vis spectroscopy. Furthermore, the bioreduction mechanism of the chloroaurate ions and the formation mechanism of the AuNPs were discussed.

Experimental details

Materials

Chloroauric acid ($HAuCl_4 \cdot 4H_2O$), β-D-glucose ($C_6H_{12}O_6$), and rutin hydrate ($C_{27}H_{30}O_{16} \cdot 3H_2O$) were purchased from Sinopharm Chemical Reagent Co. Ltd. (China). Sundried *C. Platycladi* leaf was purchased from Xiamen Jiuding Drugstore (China). Other chemicals were all purchased from commercial suppliers and used without further purification.

Preparation of *C. Platycladi* leaf extract and its simulated solution

The *C. Platycladi* leaf was milled and powdered leaf screened with a 20 mesh sieve, and 1.0 g of the sieved powder was dispersed in 100 mL deionized

water using a water bath shaker for 4 h to obtain the extract. The mixture was then filtrated to remove the residual insoluble biomass, and the resulting filtrate was used later for the synthesis of the AuNPs. The simulated solution of the active components was prepared by mixing rutin (0.255 g L^{-1}) and β-D-glucose (0.489 g L^{-1}) dissolved in deionized water.

Components measurement

The following conventional methods were adopted to measure the contents of biomolecule components of the extract before and after the reaction (Xu 2009). The content of polysaccharide was measured by phenol–sulfuric acid method. Reducing sugar content was determined using 3,5-Dinitrosalicylic acid colorimetric method. The content of protein was assayed by Coomassie Brilliant Blue method. The total flavonoid content was determined and calculated by spectrophotometry method with rutin as the standard sample. Total antioxidant activity was investigated by 2,2-diphenyl-1-picrylhydrazyl (DPPH) free radical-scavenging assay in a process regulated by its discoloration(Chen et al. 2006).

Synthesis and characterization

Biosynthesis of AuNPs was realized through a simple procedure by reducing chloroaurate acid with *C. Platycladi* leaf extract and the simulated solution. In a typical synthesis, 10 mL of the extract (or simulated solution) was added to 50 mL of Au(III) solution to make the final chloroaurate acid concentration to 1 mM. The mixing solution was then kept for 1.5 h under vigorous stirring. The temperature was controlled using a thermocouple located in a glycerin bath heater, and the pH was adjusted with dilute HCl/NaOH solutions. UV–Vis spectroscopy was carried out on a TU1900 UV–Vis spectrophotometer (Pgeneral, China). Samples for TEM were prepared by placing a drop of gold hydrosol on carbon-coated copper grids and allowing water to completely evaporate. TEM, high-resolution TEM, energy dispersive X-ray (EDX), and selected-area electron diffraction (SAED) were performed on a Tecnai F30 electron microscope (FEI, Netherlands) operated at an accelerating voltage at 300 kV. Size distribution and average size of the AuNPs were estimated by the same method as in our previous study (Huang et al. 2007). Conversion of the chloroaurate ions was determined by measuring the concentration of the residual chloroaurate ions using a TAS986 atomic absorption spectrophotometer (Pgeneral, China) after complete precipitation of the AuNPs. The extract before reaction and the resulting solution after biosynthesis of AuNPs were completely dried at 60 °C, respectively. Then, the dried biomasses were analyzed by an FTIR Nicolet Avatar 660 (Nicolet, USA). The simulated solution was treated in the same way as the leaf extract. XRD patterns of the AuNPs were recorded by an X'Pert Pro X-ray diffractometer (PANalytical BV, Netherlands) operated at a voltage of 40 kV and a current of 30 mA with Cu Kα radiation. TG were performed on a thermal analyzer TG209F1 (Netzsch, Germany) under flowing air atmosphere at a heating rate of 10 °C min^{-1} from 30 to 800 °C.

Results and discussion

Biosynthesis process by the extract

AuNPs prepared by the extract

Addition of *C. Platycladi* leaf extract to the aqueous chloroauric acid led to an abrupt color change from a pale yellow to a vivid brownish red within 5 min of reaction, indicating the formation of AuNPs. UV–Vis spectroscopy is generally acknowledged as a convenient way to examine surface plasmon resonance (SPR) of size- and shape-controlled NPs in aqueous suspensions (Wiley et al. 2006). Herein, UV–Vis spectra of the reaction solution (as a function of time) show the characteristic SPR band for AuNPs centered around 535 nm (Fig. 1) which increased in intensity with the proceeding course of the reaction. Moreover, the evolution of the absorbance spectra emanating from AuNPs over time obviously revealed that the production of AuNPs finished within 90 min after exposing the chloroauric acid to the plant extract. The results of the UV–Vis spectra were confirmed by TEM observation. Representative TEM image of the AuNPs shown in Fig. 2a indicates the formation of several well-defined spherical AuNPs. The inserted histogram in Fig. 2a shows that the AuNPs had an average particle size of 15.3 nm, with sizes ranging from 2.2 to 42.8 nm. The high-resolution TEM image and SAED

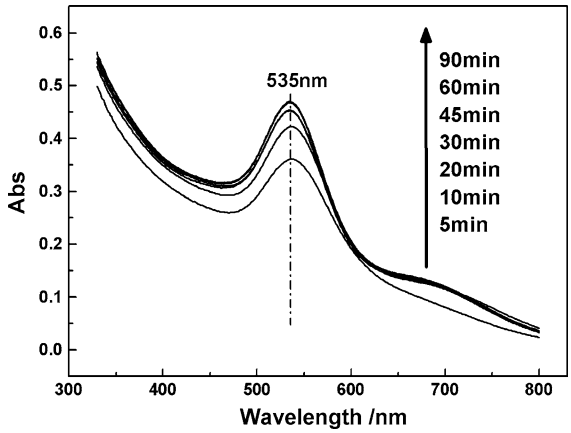

Fig. 1 UV–Vis spectra of the resulting gold hydrosol by reducing chloroaurate acid with *C. Platycladi* leaf extract (in the figure, some curves overlap with others)

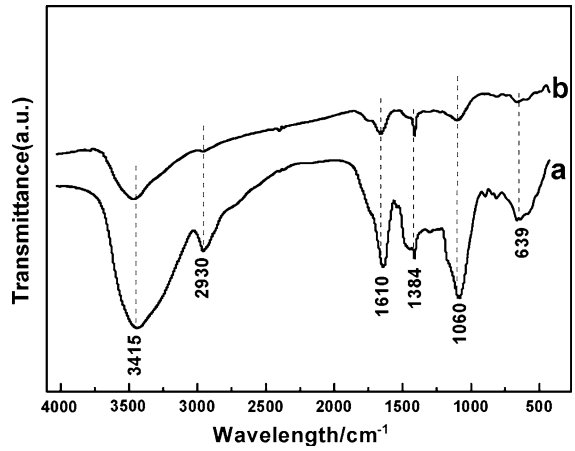

Fig. 3 Typical FTIR spectra of *C. Platycladi* leaf extract before bioreduction (**a**), and after bioreduction (**b**) of chloroaurate acid

pattern shown in Fig. 2b and c, respectively, conform to the face-centered cubic (fcc) crystalline structure of metallic gold.

FTIR and TG analyses

FTIR analysis was carried out to identify the possible functional groups responsible for the reduction of chloroauric acid and stabilization of the AuNPs. FTIR spectra of the extract (Fig. 3) reveal that six bands at 3415, 2930, 1610, 1384, 1060, and 639 cm^{-1} turn significant changes after the bioreduction. These six notable absorption peaks may be assigned to several functional groups, such as C=C–H, C–O–H, etc. The absorption bands at 2930 and 1610 cm^{-1} may be attributed to the stretching vibration of ν(=C–H) and ν(C=C), respectively, while the band nearby 639 cm^{-1} may be assigned to δ(C–H) bending vibration (Williams and Fleming 1995). Similarly, the bands at 3415 and 1384 cm^{-1} may be assigned to the stretching vibration of ν(O–H) and in-plane bending vibration of δ(O–H), respectively. Moreover, the band at 1060 cm^{-1} may have been contributed by ν(C–O). Therefore, we speculate that components containing C=C–H or C–O–H functional groups were responsible for the reduction of chloroaurate ions. In addition, FTIR spectrum of AuNPs purified after centrifuging and washing is shown in Fig. 4, displaying several absorption peaks located at 1384, 1610, and 3448 cm^{-1}. These absorption peaks are attributed to the protective biomass adhering around AuNPs which contain C=C–H and C–O–H functional groups. Simultaneously, TG analysis shown in the inset of Fig. 4 further confirms the presence of some protective

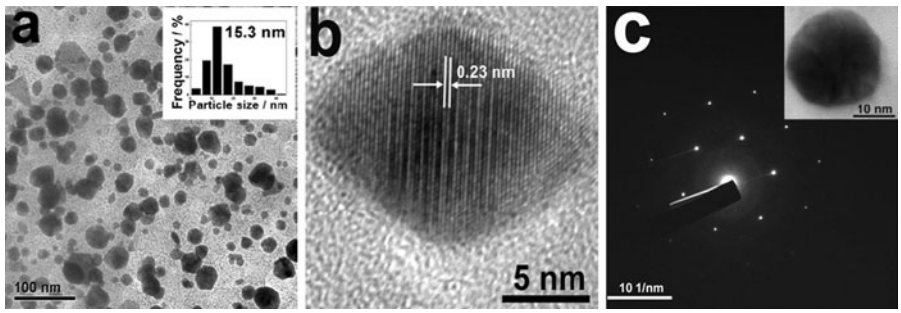

Fig. 2 Representative TEM image (**a**), high-resolution TEM image (**b**), and SAED pattern (**c**) illustrating the formation of AuNPs prepared by *C. Platycladi* leaf extract

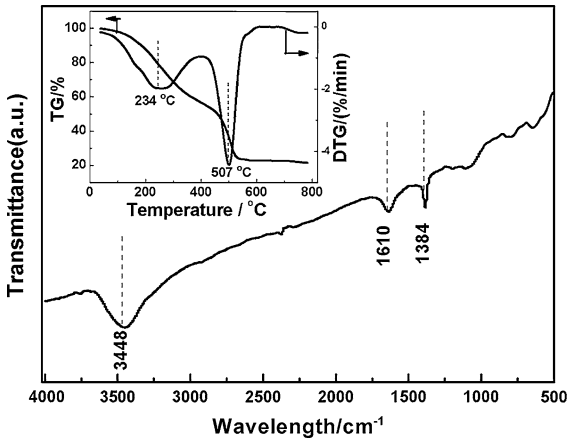

Fig. 4 Typical FTIR spectrum of the purified AuNPs prepared by *C. Platycladi* leaf extract. The *inset* shows TG and DTG analyses of the corresponding AuNPs

substances around the AuNPs. Results from differential thermogravimetric (DTG) analysis (inset of Fig. 4) prove that the decomposition temperature or gasification temperature of these protective substances were 234 and 507 °C. Hence, we speculate again that two components serve as the protective agents: one of the reasons for choosing two components for the simulation of the active components as described in the later sections. Moreover, careful TEM observations of the purified AuNPs after centrifuging and washing (shown in Fig. 5) further prove the biomass residual on the surface of AuNPs playing the role as stabilizer. All the above information implies that the components containing C=C–H and C–O–H functional groups are responsible for the formation of AuNPs, serving as both reducing and protecting agents.

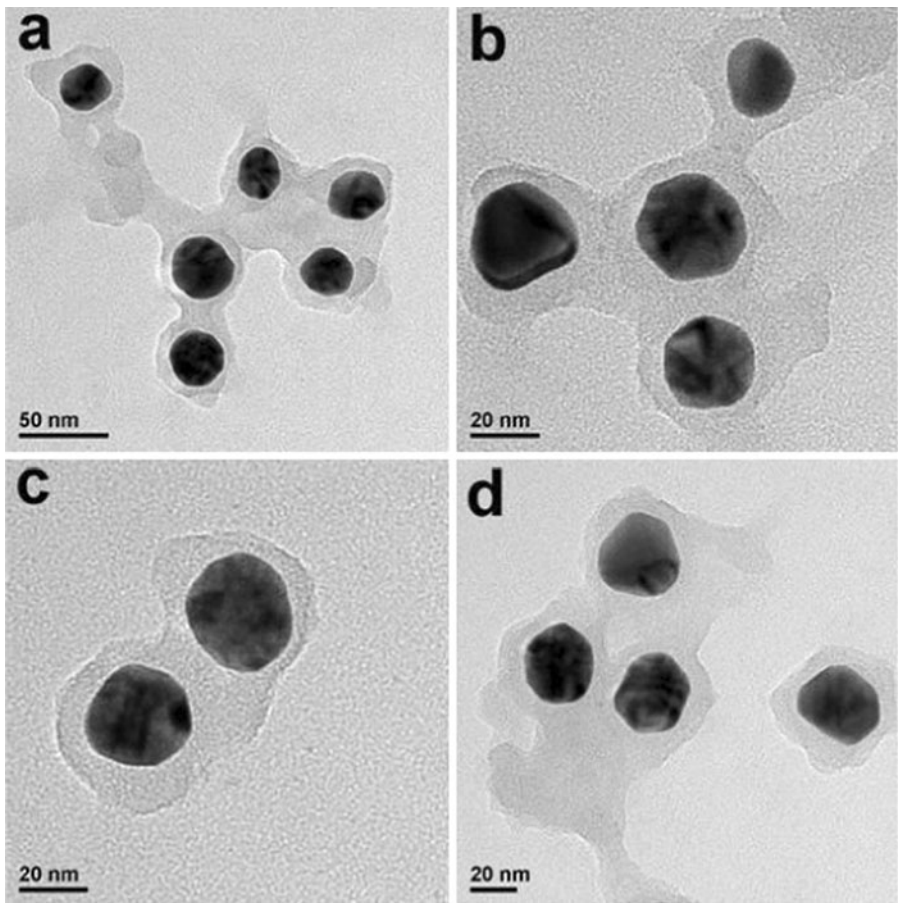

Fig. 5 Representative TEM images of the purified AuNPs after centrifuging and washing treatments revealing the biomass–AuNPs interaction. **a–d** AuNPs prepared by bioreduction of chloroaurate acid (1 mM) with *C. Platycladi* leaf extract at 20 °C. Scale bar: **a** 50 nm; **b–d** 20 nm

Variances of main components of the extract before and after reaction

In order to further identify the active biomolecules responsible for the reduction of Au(III) to Au(0), the biomolecule components of the extract before and after the reaction were tested by those methods mentioned above. The results (listed in Table 1) give clear information that the amount of polysaccharide, reducing sugar, total protein, total flavonoid, and total antioxidant capability decreased after the reaction, especially, in terms of the total antioxidant capability. Antioxidants have strong reducing ability; they donate electrons to convert Au(III) into Au(0) resulting in their high variation. Total flavonoid and reducing sugar had the most noticeable changes among the components suggesting that they may be responsible for the reduction of the chloroauric acid. Combining this idea with the FTIR and TG analyses, we speculate that the active biomolecules responsible for the biosynthesis of the AuNPs are flavonoid and reducing sugar, which widely exist in plant biomass. To validate this claim, a simulated solution of these active components (flavonoid and reducing sugar) was prepared for evaluation. Herein, rutin and β-D-glucose (Fig. 6) were chosen to represent the flavonoid and reducing sugar, respectively. Both rutin and β-D-glucose are widely distributed in plants, and they are proved as two components in *C. Platycladi* leaf (Chen and Liu 2008; Zhou et al. 2004). The applied formula of the simulated solution was based on the amount of each in the *C. Platycladi* leaf extract (see Table 1): 0.489 g L^{-1} for β-D-glucose and 0.255 g L^{-1} for rutin. This new simulated solution was adopted to synthesize AuNPs, and the

Table 1 Components variance of *C. Platycladi* leaf extract before and after the reaction

Components	Before reaction	After reaction	Change (%)
Polysaccharide	0.725 g/L	0.677 g/L	6.60
Reducing sugar	0.489 g/L	0.247 g/L	49.4
Total protein	0.097 g/L	0.086 g/L	10.7
Total flavonoid	0.255 g/L	0.185 g/L	27.4
Total antioxidant capability (%)[a]	43.8	10.4	76.3

[a] Total antioxidant capability is not a specific composition of the plant extract and the value was determined by 80 mg/L DPPH free radical-scavenging rate

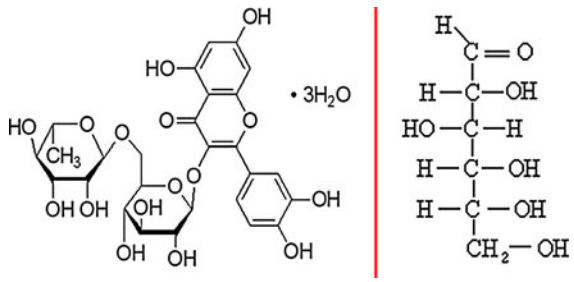

Fig. 6 The structural formula of rutin hydrate (*left*) and β-D-glucose (*right*)

influences of temperature and pH upon the synthetic process were investigated. Finally, the comparison between the extract and its simulated solution was also carried out.

Influencing factors on synthesis of AuNPs

Influence of temperature

First, the effect of temperature on the synthesis of AuNPs by simulated solution was investigated. With constant aqueous chloroauric acid and pH (initial pH value of about 3.3), comparative experiments were carried out to investigate the effect of temperature on sizes of the resulting AuNPs. Five different reaction temperatures were chosen: 30, 45, 60, 75, and 90 °C. These generations of AuNPs were validated by their TEM images (Fig. 7a–e). The size distributions of the AuNPs are shown in the insets of these images, revealing that the size variation had a negative relationship with the reaction temperature. It was found that the AuNPs prepared at 30 °C was larger than 200 nm due to agglomeration. On the contrary, at 90 °C, the mean size of the AuNPs was 115 nm. Figure 7f shows the UV–Vis absorption spectra of the AuNPs produced at different reaction temperatures. While no absorption band was observed from the sample obtained at 30 °C, characteristic SPR bands centered at 564 nm were observed from the other four samples (synthesized at 45, 60, 75, and 90 °C). Moreover, the effect of temperature upon the synthetic process by the plant extract itself was also investigated. Figure 8 displays the UV–Vis spectra and the mean particle size of AuNPs synthesized by the extract at different reaction temperatures. Evidently, the average size of the AuNPs decreased, and the size distribution became narrower as the reaction temperature increases. Higher reaction temperature

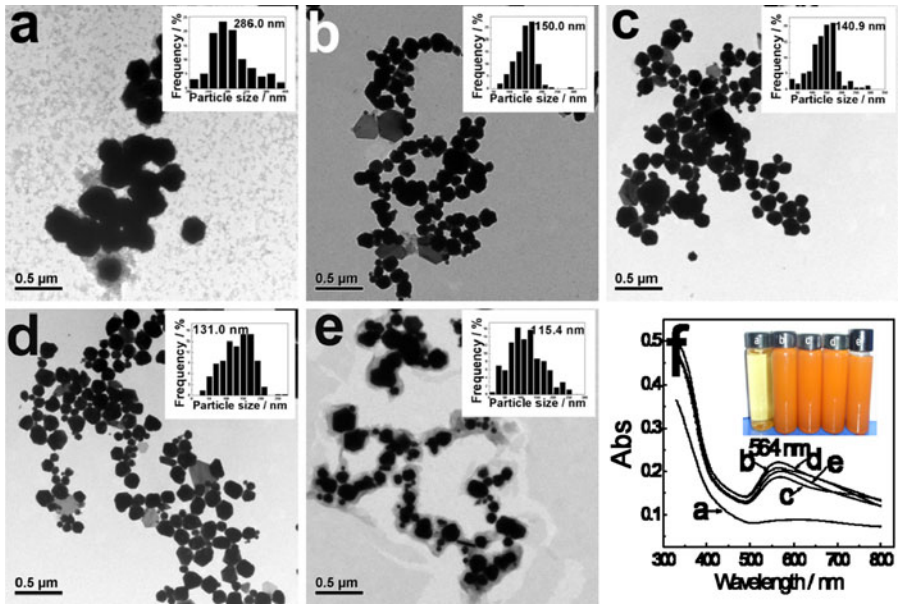

Fig. 7 Typical TEM images and the corresponding size distributions of AuNPs synthesized at different reaction temperature of **a** 30, **b** 45, **c** 60, **d** 75, and **e** 90 °C. **f** UV–Vis spectra recorded from the corresponding reaction solutions at 90 min; *inset* is the photo taken from gold hydrosols under different reaction temperature whose labels correspond to TEM images

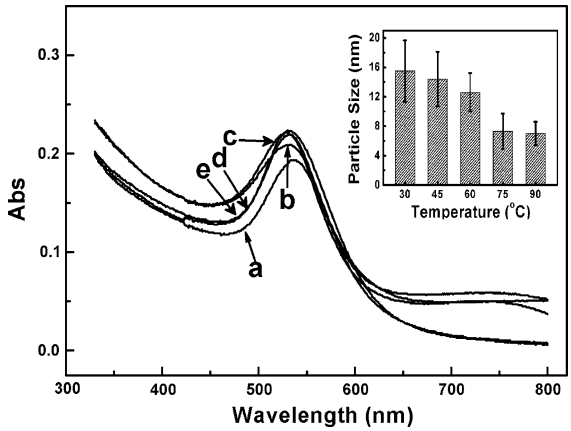

Fig. 8 UV–Vis spectra recorded from AuNPs synthesized by *C. Platycladi* leaf extract at different reaction temperature of (*a*) 30, (*b*) 45, (*c*) 60, (*d*) 75, and (*e*) 90 °C. *Inset* shows the corresponding mean particle size of AuNPs

led to a rapid reduction rate of the chloroaurate ions and the subsequent homogeneous nucleation of gold nucle—allowing for the formation of AuNPs with small size and narrow size distribution.

Influence of pH of the reaction solution

After studying the influence of temperature, the effects of different pH values (2, 4, 7, 10, and 12) of the simulated solution on the synthesis of the AuNPs were also investigated. Likewise, the size and shape of the AuNPs were checked by TEM (Fig. 9a–e). It is seen from these images that pH had a significant effect on the property of the obtained AuNPs. The size of the AuNPs decreased with increasing pH. Figure 9f shows the SPR bands of AuNPs centered at very different wavelengths under different pH values. The intensity of the absorbance peaks increased, and the SPR bands shifted gradually from 554 to 534 nm with the increasing pH. The blue shift also indicates the decreasing size of the AuNPs. Furthermore, AuNPs synthesized by chemical methods (without templates) are generally spherical, and other morphologies are rare. Nevertheless, our results showed AuNPs with diversity of spheres, triangles, truncated triangles, and hexahedrons morphologies at pH values of 4 (Fig. 9b) and 7 (Fig. 9c). The reaction between active biomolecules and the Au anionic species may have the following relationship:

$$n\,\mathrm{Au(III)} + 3\mathrm{H_nR} \rightarrow n\,\mathrm{Au(0)} + 3\,\mathrm{R'} + 3n\,\mathrm{H^+} \qquad (1)$$

where H_nR and R' represent the active biomolecules, and n represents the number of electrons donated by the biomolecules to Au(III). Thus, biomolecules were oxidized, whereas Au(III) was reduced. From the reaction stoichiometry, the redox reaction includes the transfer of three electrons and three protons, which indicate that both the kinetics and the standard redox potentials may be pH dependent. High pH leads to rapid reduction rate of the chloroaurate ions,

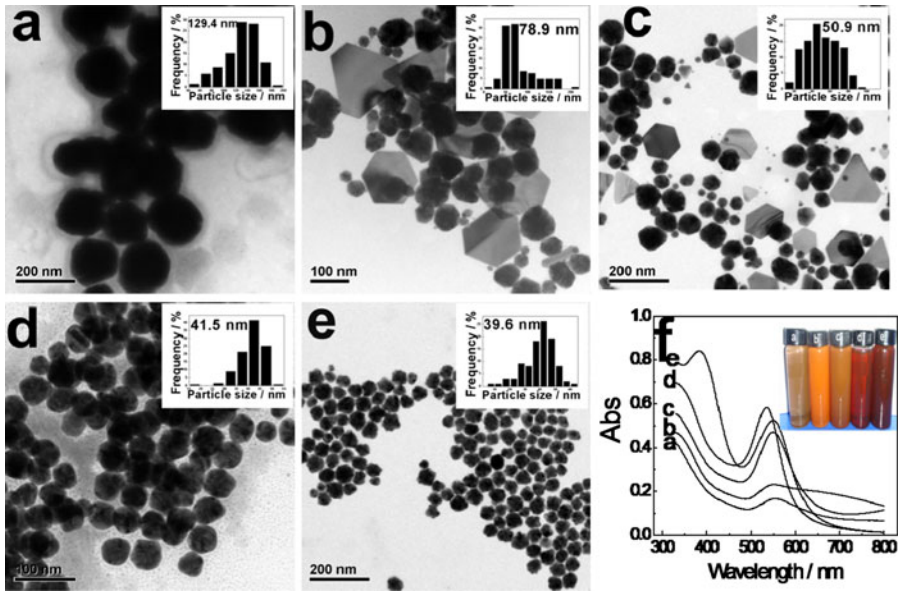

Fig. 9 Typical TEM images and the corresponding size distributions of AuNPs produced at 60 °C under different pH values of reaction solutions of **a** 2, **b** 4, **c** 7, **d** 10, and **e** 12. **f** UV–Vis spectra recorded from the corresponding reaction solutions at 90 min; *inset* is the photo taken from gold hydrosols under different pH values of reaction solution whose labels correspond to TEM images

boosts the homogenous nucleation, and decreases in anisotropy growth. In contrast, slow reduction rate would occur under acidic condition resulting in the heterogeneous nucleation and secondary nucleation of small Au seeds. In addition, at a high pH, the AuNPs tend to have more negative charge by adsorption of hydroxide anions at the particles surface, giving rise to electrostatic repulsion between the AuNPs—stabilizing them without aggregation. In other words, the use of simulated solution may be a new way to regulate the shape of AuNPs by merely varying the pH value of the reaction solution. Likewise, Fig. 10 shows the UV–Vis spectra of the colloidal gold obtained by the extract under different pH conditions showing a similar phenomenon to that of the simulated solution.

Comparison between the extract and the simulated solution

The comparison of the formed AuNPs

Comparative experiments between the leaf extract and the simulated solution of the active components were carried out to demonstrate the success of the simulation and to elucidate the mechanism of the biosynthesis process. Considering that the simulated solutions were able to synthesize AuNPs under basic

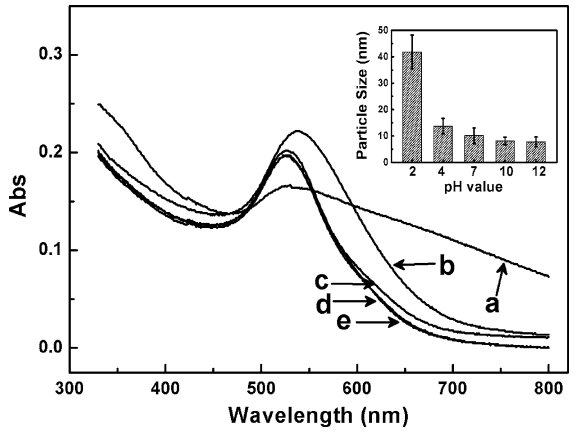

Fig. 10 UV–Vis spectra recorded from AuNPs synthesized by *C. Platycladi* leaf extract at 60 °C under different pH values of reaction solutions of (*a*) 2, (*b*) 4, (*c*) 7, (*d*) 10, and (*e*) 12. *Inset* shows the corresponding mean particle size of AuNPs

condition, we controlled the pH of the comparative reaction solutions to 10 and examined their bioreduction capabilities. Parameters examined are conversion of chloroaurate ions, mean size, size distribution, and morphology of the AuNPs. Figure 11 shows the UV–Vis spectra recorded from the time courses of colloidal gold prepared by the simulated solution. The characteristic SPR band of AuNPs was quite similar to that of the leaf extract (Fig. 1). In order to understand the conversion of chloroaurate ions, AAS (Fig. 12) was

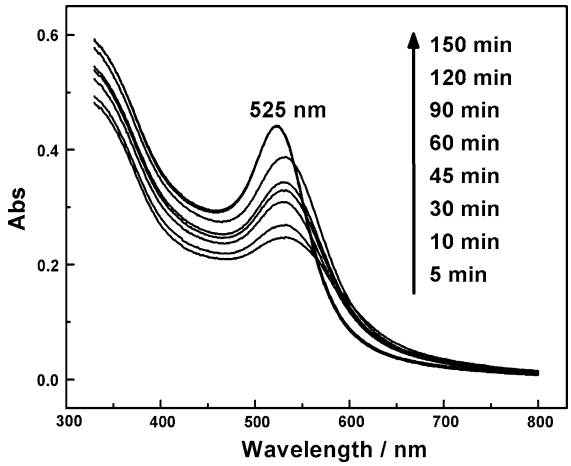

Fig. 11 UV–Vis spectra of the resulting gold hydrosol by reducing chloroaurate acid with simulated active components at 20 °C (the pH value of the reaction solution was 10). The *curves* representing 120 and 150 min overlap with each other

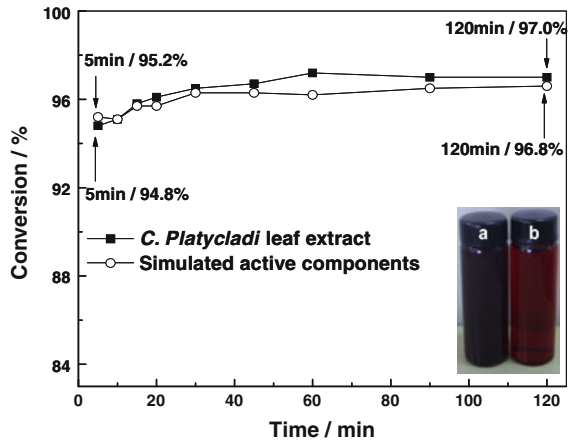

Fig. 12 The time-conversion plot for chloroaurate ions reduction with *C. Platycladi* leaf extract (*filled square*) and its simulated active components (*open circle*). The *inset* is the photo taken from gold hydrosols by *C. Platycladi* leaf extract (*a*) and its simulated active components (*b*)

employed. Greater than 95% conversion of chloroaurate ions was achieved within 5 min by the simulated solution, almost equal to that of the leaf extract. The corresponding TEM image and size distribution of the AuNPs prepared by the simulated solutions are displayed in Fig. 13a, with mean size of 18.6 ± 1.8 nm. As shown, majority of the AuNPs were spherical and appeared to be reasonably monodispersive. High-resolution TEM image and SAED pattern of the AuNPs are shown in Fig. 13b and c, respectively. EDX analysis is shown in Fig. 13d where the Au element signal is indicated. Consequently, the AuNPs prepared with the two solutions (leaf extract and simulated) indeed had comparable properties (confirmed by the mean size, size distribution, dispersity, and morphology studies). Figure 14 shows the XRD patterns of the AuNPs prepared by the leaf extract and its simulated solution, respectively. The two XRD patterns revealed that both types of AuNPs corresponded to the crystalline gold fcc phase. According to the intensity ratio between (200) and (111) diffraction peaks, we could learn that the (111) plane was the predominant orientation in the gold crystal structure of both types of AuNPs (Kannan and John 2008). Hence, the simulated solution exhibited excellent performance on the synthesis of AuNPs as that of the plant extract.

The comparison of bioreduction mechanism

Further to the above analyses, FTIR measurements were carried out to identify the possible functional groups responsible for the biosynthesis of AuNPs by the simulated solution. The marked changes of the absorption bands in FTIR spectra (Fig. 15) before and after reaction correspond to the C=C–H and C–O–H functional groups. Comparing the FTIR spectra of the leaf extract with those of the simulated solution (Fig. 16), it is clear that the two solutions have similar composition, as their individual spectra have almost the same absorption bands between 400 and 4000 cm^{-1}. Moreover, Fig. 17 shows FTIR spectra of the AuNPs purified after centrifuging and washing, revealing good agreement with the fact that those protective substances adhered around AuNPs. The inset of Fig. 17 shows TG analyses of the AuNPs prepared from the two solutions. The residual mass fraction of the AuNPs from the simulated solution after heating up to 800 °C was 36.2%. However, that of the AuNPs from the leaf extract was 21.4% indicating that the amount of protective substances from the simulated solution was lesser than that of the leaf extract. This may be assigned to the simple nature of the simulation (ignoring small and insignificant components). Although the simulation is oversimplified, it allows for the exploration of plausible biosynthesis mechanism, and the results obtained above apparently demonstrate the success.

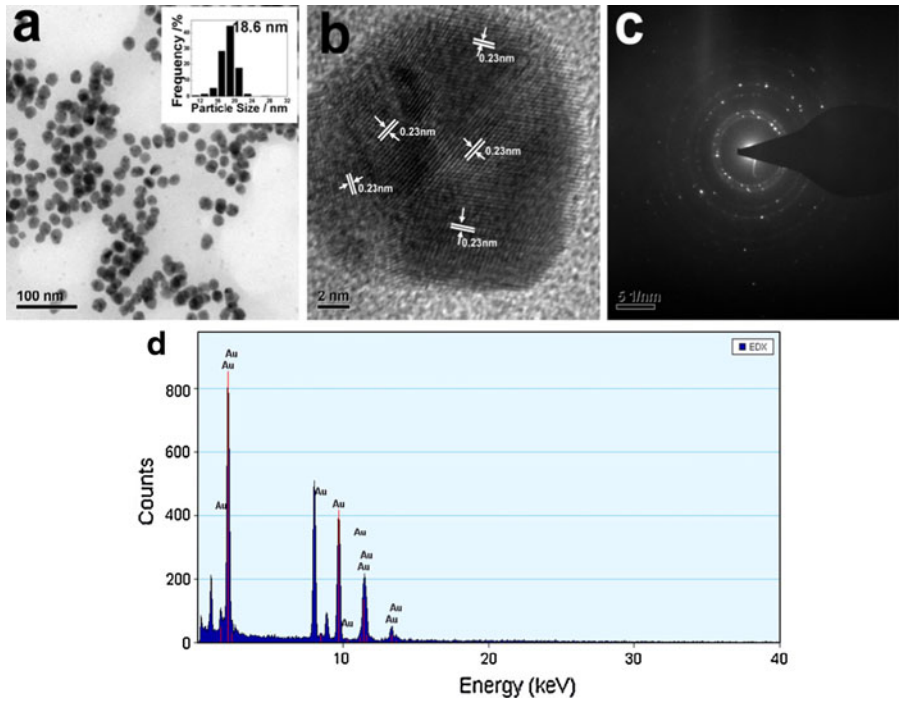

Fig. 13 TEM image (**a**), high-resolution TEM image (**b**), SAED pattern (**c**), and EDX spectrum (**d**) illustrating the formation of AuNPs prepared by simulated active components at 20 °C (the pH value of the reaction solution was 10)

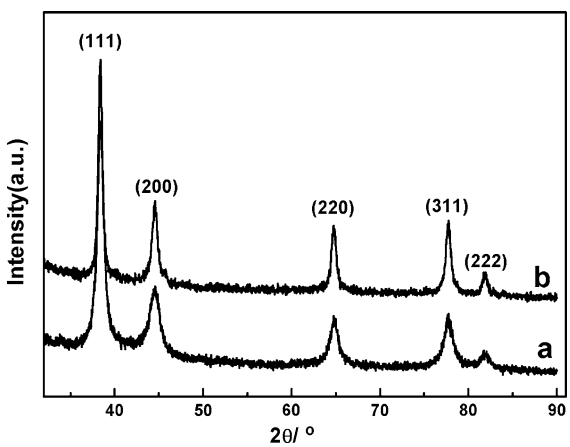

Fig. 14 XRD patterns of AuNPs prepared by reducing chloroaurate acid with *C. Platycladi* leaf extract (*a*) and its simulated active components (*b*) at 20 °C

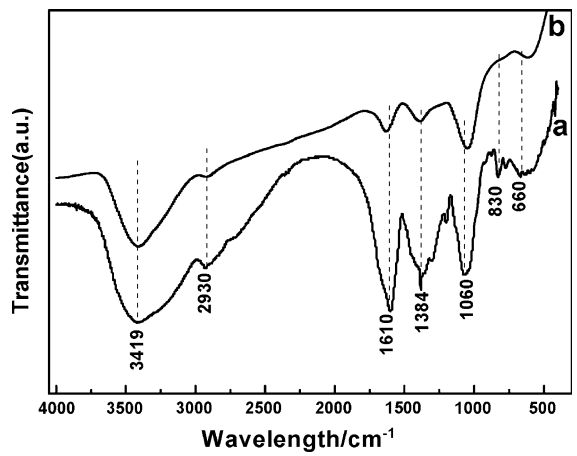

Fig. 15 Typical FTIR spectra of simulated active components before reaction (*a*) and after reaction (*b*) as the pH value of the solution being adjusted to 10

Conclusions

In summary, biogenic fabrication of AuNPs by *C. Platycladi* leaf extract and its simulated solution were investigated to understand the plant-mediated biosynthetic mechanism. The results showed that the simulated solution exhibited excellent performance on the synthesis of the AuNPs comparable to that of the plant extract. Based on the analyses, we conclude that flavonoid and reducing sugar are the main categories of the ingredients in *C. Platycladi* leaf extract serving as both reducing and protecting agents for AuNPs. Moreover, pH of the reaction solution was the most critical factor upon the synthesis process with the simulated solution. We therefore propose that the use of simulated solution represents an important protocol for the exploration of the biosynthesis mechanism.

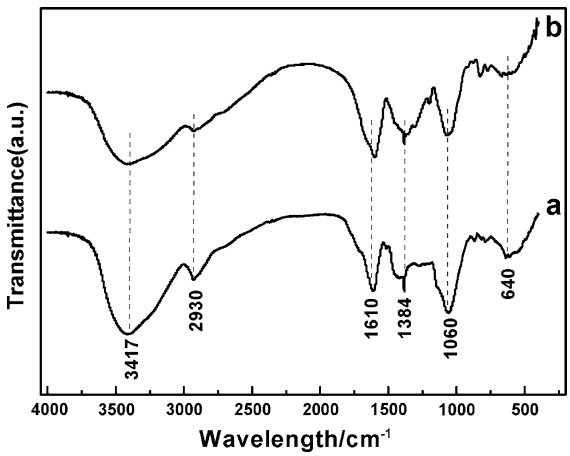

Fig. 16 The comparison of FTIR spectra between *C. Platycladi* leaf extract (*a*) and its simulated active components (*b*)

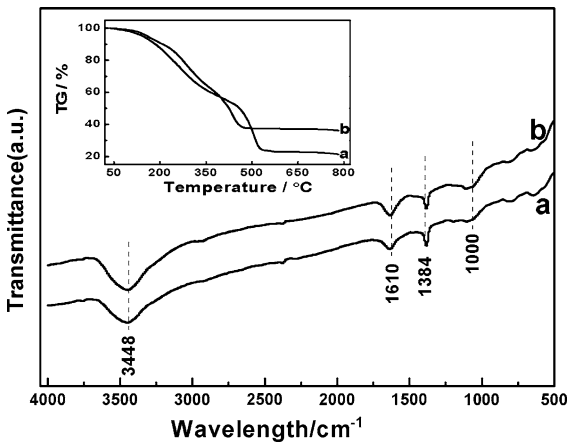

Fig. 17 Typical FTIR spectra of the purified AuNPs prepared by with *C. Platycladi* leaf extract (*a*) and its simulated active components (*b*). The *Inset* shows TG analyses of the corresponding AuNPs

Acknowledgments This study was supported by the key program (No. 21036004) and general program (Nos. 20776120, 20976146, and 30700020) of the National Natural Science Foundation of China, the Natural Science Foundation of Fujian Province of China (Grant Nos. 2010J05032 and 2010J01052), and the Fundamental Research Funds for the Central Universities (No. 2010121051).

References

Ankamwar B, Damle C, Ahmad A, Sastry M (2005) Biosynthesis of gold and silver nanoparticles using Emblica officinalis fruit extract, their phase transfer and transmetallation in an organic solution. J Nanosci Nanotechnol 5:1665–1671

Anuradha J, Tasneem A, Abbasi SA (2010) 'Green' synthesis of gold nanoparticles with aqueous extracts of Neem (Azadirachta indica). Res J Biotechnol 5:75–79

Armendariz V, Jose-Yacaman M, Moller AD, Peralta-Videa JR, Troiani H, Herrera I, Gardea-Torresdey JL (2004) HRTEM characterization of gold nanoparticles produced by wheat biomass. Rev Mex Fis 50:7–11

Brust M, Bethell D, Kiely CJ, Schiffrin DJ (1998) Self-assembled gold nanoparticle thin films with nonmetallic optical and electronic properties. Langmuir 14:5425–5429

Chandran SP, Chaudhary M, Pasricha R, Ahmad A, Sastry M (2006) Synthesis of gold nanotriangles and silver nanoparticles using Aloe vera plant extract. Biotechnol Prog 22:577–583

Chen FK, Liu XQ (2008) Determination of active components of traditional Chinese medicine. People's Medical Publishing House, Beijing

Chen FA, Wu AB, Shieh P, Kuo DH, Hsieh CY (2006) Evaluation of the antioxidant activity of *Ruellia tuberosa*. Food Chem 94:14–18

Daniel MC, Astruc D (2004) Gold nanoparticles: assembly, supramolecular chemistry, quantum-size-related properties, and applications toward biology, catalysis, and nanotechnology. Chem Rev 104:293–346

Fitz-Gerald J, Pennycook S, Gao H, Singh RK (1999) Synthesis and properties of nanofunctionalized particulate materials. Nanostruct Mater 12:1167–1171

Gardea-Torresdey JL, Tiemann KJ, Gamez G, Dokken K, Tehuacanero S, Jose-Yacaman M (1999) Gold nanoparticles obtained by bio-precipitation from gold(III) solutions. J Nanopart Res 1:397–404

Gericke M, Pinches A (2006) Microbial production of gold nanoparticles. Gold Bull 39:22–28

Huang J, Li Q, Sun D, Lu Y, Su Y, Yang X, Wang H, Wang Y, Shao W, He N, Hong J, Chen C (2007) Biosynthesis of silver and gold nanoparticles by novel sundried Cinnamomum camphora leaf. Nanotechnology 18:105104

Jin RC, Cao YW, Mirkin CA, Kelly KL, Schatz GC, Zheng JG (2001) Photoinduced conversion of silver nanospheres to nanoprisms. Science 294:1901–1903

Kannan P, John SA (2008) Synthesis of mercaptothiadiazole-functionalized gold nanoparticles and their self-assembly on Au substrates. Nanotechnology 19:085602

Kasthuri J, Kathiravan K, Rajendiran N (2009) Phyllanthin-assisted biosynthesis of silver and gold nanoparticles: a novel biological approach. J Nanopart Res 11:1075–1085

Labrenz M, Druschel GK, Thomsen-Ebert T, Gilbert B, Welch SA, Kemner KM, Logan GA, Summons RE, De Stasio G, Bond PL, Lai B, Kelly SD, Banfield JF (2000) Formation of sphalerite (ZnS) deposits in natural biofilms of sulfate-reducing bacteria. Science 290:1744–1747

Liu B, Xie J, Lee JY, Ting YP, Chen JP (2005) Optimization of high-yield biological synthesis of single-crystalline gold nanoplates. J Phys Chem B 109:15256–15263

Lopez ML, Parsons JG, Videa JRP, Gardea-Torresdey JL (2005) An XAS study of the binding and reduction of Au(III) by hop biomass. Microchem J 81:50–56

Lu XM, Yavuz MS, Tuan HY, Korgel BA, Xia YN (2008) Ultrathin gold nanowires can be obtained by reducing polymeric strands of oleylamine-AuCl complexes formed

via aurophilic interaction. J Am Chem Soc 130:8900–8901

Mohanpuria P, Rana NK, Yadav SK (2008) Biosynthesis of nanoparticles: technological concepts and future applications. J Nanopart Res 10:507–517

Narayanan KB, Sakthivel N (2008) Coriander leaf mediated biosynthesis of gold nanoparticles. Mater Lett 62:4588–4590

Pal A, Shah S, Devi S (2007) Preparation of silver, gold and silver-gold bimetallic nanoparticles in w/o microemulsion containing TritonX-100. Colloid Surf A 302:483–487

Shankar SS, Ahmad A, Pasricha R, Sastry M (2003a) Bioreduction of chloroaurate ions by geranium leaves and its endophytic fungus yields gold nanoparticles of different shapes. J Mater Chem 13:1822–1826

Shankar SS, Ahmad A, Sastry M (2003b) Geranium leaf assisted biosynthesis of silver nanoparticles. Biotechnol Prog 19:1627–1631

Shankar SS, Rai A, Ankamwar B, Singh A, Ahmad A, Sastry M (2004) Biological synthesis of triangular gold nanoprisms. Nat Mater 3:482–488

Shipway AN, Katz E, Willner I (2000) Nanoparticle arrays on surfaces for electronic, optical, and sensor applications. ChemPhysChem 1:18–52

Singh AK, Talat M, Singh DP, Srivastava ON (2010) Biosynthesis of gold and silver nanoparticles by natural precursor clove and their functionalization with amine group. J Nanopart Res 12:1667–1675

Wiley BJ, Im SH, Li ZY, McLellan J, Siekkinen A, Xia YA (2006) Maneuvering the surface plasmon resonance of silver nanostructures through shape-controlled synthesis. J Phys Chem B 110:15666–15675

Williams DH, Fleming I (1995) Spectroscopic methods in organic chemistry. The McGraw-Hill, New York

Xia Y, Xiong YJ, Lim B, Skrabalak SE (2009) Shape-controlled synthesis of metal nanocrystals: simple chemistry meets complex physics? Angew Chem Int Ed 48:60–103

Xu J (2009) Experiment and guide for biochemistry. China Medical Science and Technology Press, Beijing

Yu DB, Yam VWW (2005) Hydrothermal-induced assembly of colloidal silver spheres into various nanoparticles on the basis of HTAB-modified silver mirror reaction. J Phys Chem B 109:5497–5503

Zhou JJ, Xie GR, Yan JX (2004) Traditional Chinese medicine: molecular structure natural source. Chemical Industry Press, Beijing